

# Experimental analysis and performance of a 5-cells HT-PEMFC stack under induced starvation of reactant gases

C. Alegre<sup>1</sup>, A. Lozano<sup>1</sup>, A. Pérez Manso<sup>2</sup>, L. Álvarez-Manuel<sup>1</sup>, F. Fernández<sup>2</sup>, F. Barreras<sup>1,\*</sup>

<sup>1</sup> LIFTEC, CSIC-Univ. of Zaragoza, C/ María de Luna, 10. 50018, Zaragoza (SPAIN)

<sup>2</sup> Escuela de Ingeniería de Guipúzcoa, University of the Basque Country, UPV-EHU, Plaza de Europa, 1. 200018, San Sebastián (SPAIN)

(\*) Corresponding author: [felix@litec.csic.es](mailto:felix@litec.csic.es)

---

**Keywords:** PEM fuel cell; high temperature; starvation; MEA degradation

---

## 1. Introduction

Even though during the last few years important progress has been achieved, the lifetime of HT-PEMFCs under variable load conditions needs to be enhanced. Performance degradation during HT-PEMFCs lifetime, operating with phosphoric acid doped-PBI membranes, is due to two main factors: reduction of the catalyst active area and phosphoric acid migration [1]. Since lifetime tests are impractical due to their long duration, several accelerated stress test protocols have been usually employed [2,3]. A phenomenon that has a significant impact on the performance deterioration of PEMFCs is the starvation of reactant gases, which can induce strong degradation in the catalyst layers due to the corrosive potentials that can be reached. However, very few studies have been focused on HT-PEM fuel cells, and most of them are concerned on phosphoric acid fuel cells (PAFC) or in single cells.

The present research is aimed to analyze the effect of the induced starvation of reactant gases on the performance and degradation of the starving cell and its neighbors. A specifically designed 5-cell stack was used, which enables controlled variations of the gas supplied to any of the individual cells. Two types of tests were performed acting on cell 3 (central) denoted as moderate and severe starvation, respectively. The difference between them depended on the intensity of the limitation imposed to the gases flowrate. During the tests the voltage of each cell was continuously monitored.

## 2. Experimental

### 2.1 Stack design and assembly

The stack consists of 5 cells with individual gas supply to each one of them. It is formed by 6 graphite plates and two end plates of stainless steel where all the connectors for the reactant gases ( $H_2$  and  $O_2$ ) are placed. Commercial high-temperature membrane-electrode assemblies (MEAs) of  $H_3PO_4$  doped PBI manufactured by Danish Power System (DPS) with a rectangular active area of  $163.5\text{ cm}^2$ , were used. The recommended working temperature ranges from  $150^\circ\text{C}$  to  $170^\circ\text{C}$ . The bipolar plates were manufactured by Mersen in JP-945 graphite, suitable for working temperatures up to  $200^\circ\text{C}$ . The flowfield geometry in both anode and cathode sides consisted of straight parallel channels with a land-to-channel ratio of 1, as recommended by the MEA manufacturer.

One of the aims of the designed stack was to vary independently the gas flow supplied to each cell in order to study the influence of gas starvation on the performance of the starving cell and its neighbors. For this reason, 10 low pressure micrometric valves were used for an efficient control of the gas flow. To ease the operation during the tests, the 5 valves used for the supply of each reactant gas ( $H_2$  and  $O_2$ ), were assembled in separate racks. In order to know the exact gas flow supplied, an accurate calibration of the flow rate was performed using the mass flow controllers of the dual test bench of the LIFTEC. The flow was changed varying the number of turns of the micrometric screw in the valves for different inlet gas pressures.

### 2.2 Experimental setup

All the experimental tests were performed in the dual test bench. The stack was heated using two Roweld Quick S industrial air heaters, which can reach air temperatures up to  $700^\circ\text{C}$ . To minimize the heating

time, and to ensure a homogeneous heating, the stack was placed inside a box formed by 5 plates of a thermal insulating material, leaving its front part open. The temperature of the different plates of the stack was measured using a thermal infrared FLIR T-200 camera. The experimental assembly is shown in the two photos of Fig. 1. To control the stack operation, it was connected to an IT-8514-F dynamic electronic load. In order to reach a higher performance of the MEAs, the breaking procedure recommended by DPS was followed during 24 hours.



Figure 1. Experimental setup of the 5-cell stack in the dual test bench

To perform the experimental tests, the stack was initially heated up with the two industrial air heaters, and once a temperature of  $140^{\circ}\text{C}$  was reached, reactant gases flowrates were established to  $0.7 \text{ NI min}^{-1}$  for  $\text{H}_2$  and  $0.4 \text{ NI min}^{-1}$  for  $\text{O}_2$ , respectively. After that, a current of  $16.35 \text{ A}$  was demanded during 10 minutes, in order to ensure a constant delivered voltage and a constant working stack temperature of  $160^{\circ}\text{C}$ . Subsequently, the current was increased stepwise to reach  $32.7 \text{ A}$  ( $0.2 \text{ A/cm}^2$ ), adjusting the reactant gases flowrates to the corresponding values for a stoichiometry of 1.15 for hydrogen and 1.25 for oxygen. It is important to note that the performance of the stack was analyzed under steady-state conditions just before and after the induced starvation tests. In these tests, the demanded current was kept constant at  $32.7 \text{ A}$ , and an average working temperature of  $160^{\circ}\text{C}$  was also established.

### 3. Results and Discussion

To verify how the performance of the experimental stack is affected by a gas defect (starvation) and if the induced effect propagates to the neighboring cells, two tests were performed acting on cell 3 (central) denoted as “moderate starvation”, and “severe starvation”, depending on the intensity of the limitation imposed to the gases flowrate.

#### 3.1 Moderate starvation of the reactant gases induced in the central cell

To induce the “moderate starvation” of reactant gases to cell 3 (central), the flowrate was limited to 80% of that corresponding to stoichiometric flow conditions ( $\lambda_{\text{H}_2}=\lambda_{\text{O}_2}=1$ ) for the demanded current of  $32.7 \text{ A}$ . Thus, the flow of hydrogen to cell 3 was set to  $0.2 \text{ NI min}^{-1}$  ( $0.25 \text{ NI min}^{-1}$  for the rest of cells) and  $0.10 \text{ NI min}^{-1}$  for oxygen ( $0.13 \text{ NI min}^{-1}$  for the rest of cells). The total duration of the test was almost 2 hours, but the time during which cell 3 remained under gas starvation was 30 minutes. After this time, the valve of both gases was opened, passing again 100% of the stoichiometric flow to this cell. Results obtained can be seen in Fig. 2a). Due to the reactant gases starvation, the voltage of cell 3 slowly decreased by 16.4%, from  $0.725 \text{ V}$  to  $0.606 \text{ V}$ . However, when the nominal value of the flowrate for the two reactant gases was re-established, the cell gradually recovered its optimal performance, generating a voltage of  $0.722 \text{ V}$  at the end of the test. So, it can be concluded that the effects caused by a moderate starvation of the reactant gases in a cell are reversible. Besides, the behavior of the rest of the cells was scarcely affected during the test.

For HT-PEMFCs with PBI membranes, the potential shift of the cell during the starvation process is due to the reduction of the partial pressure of reactant gases on the catalyst surface, which increases the resistance for mass transport and therefore the anode potential. Under these operating conditions (low membrane humidity and high working temperature) the orthophosphoric acid (or simply phosphoric) is transformed into pyrophosphoric acid. The formation of different species of pyrophosphoric acid modifies the proton conductivity of the polymer and, therefore, the overall performance of the stack decreases. However, once the gas flowrate is restored to the nominal value, the production of water in the cathode is intensified, and the partial pressure of the water vapor increases. Finally, the water vapor is transported to the anode side by the concentration gradient, reaching the optimal humidity degree in the membrane, and eventually improving its proton conductivity.

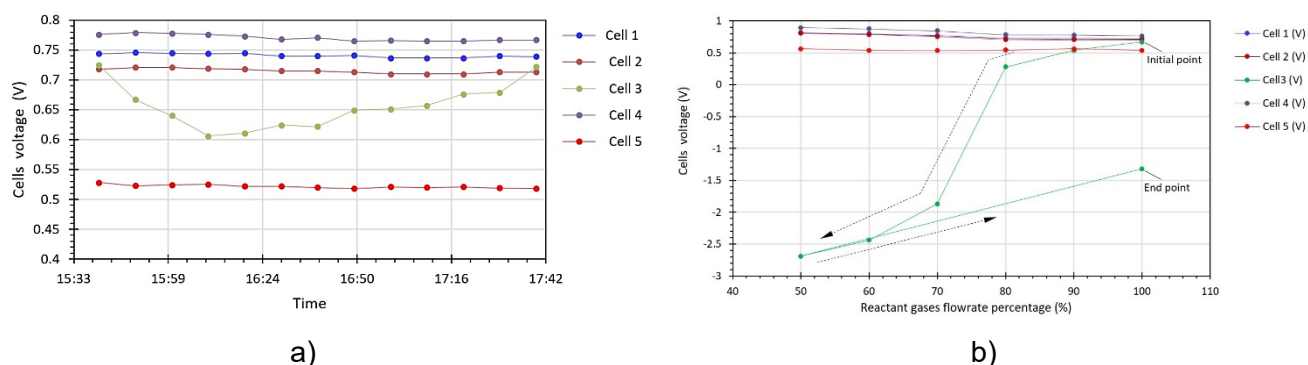


Figure 2. Voltage of the different cells under moderate starvation test (a) and severe starvation test (b)

### 3.2 Severe starvation of the reactant gases induced in the central cell

For the "severe starvation" tests, the flowrate of reactant gases was reduced from 100% to 50% in 10% steps as shown in Fig. 2b). The cell operated for 15 minutes in each one of these steps. In the final condition (50% of the flow) the cell was maintained in operation for 30 minutes, and after this time the flowrate of both gases was set again to 100%. It is also important to note that this test was performed the day after the "moderate starvation" one. It was observed that as soon as the gas flow was reduced to 90%, the voltage of cell 3 dropped to 0.54 V, while for 80% the voltage was limited to only 0.278 V. This is a poorer performance than that measured the day before during the "moderate starvation" test for the same gas flowrate limitation, probably due to the MEA degradation caused by the gas starvation. For further flowrate reductions (70%, 60%, and 50%), the voltage of cell 3 became eventually inverted, reaching a final value of  $-2.69$  V. It is also notorious that the voltage produced by the rest of the cells was not affected. On the contrary, as the voltage produced by cell 3 decreased due to the gas starvation, the voltage generated by the rest of the cells slightly increased. This unexpected performance can be explained because the current produced by the stack was significantly reduced when the potential was inverted and, consequently, the voltages of the unaffected cells increased to match the one corresponding to the actual yielded current. For example, for 70% flow, the current value was reduced to 15.5 A, for 60% it dropped to 8.72 A, while with a flowrate corresponding to 50% it only generated 4.5 A. In addition, when the flowrate of the reactant gases returned to 100% ( $0.25$  NI  $\text{min}^{-1}$  for  $\text{H}_2$ , and  $0.13$  NI  $\text{min}^{-1}$  for  $\text{O}_2$ ), the voltage of this cell remained inverted ( $-1.315$  V) and the current produced was limited to 18.6 A, 56.9% lower than the initial value (32.7 A).

## 4. Conclusions

Some relevant and novel results were obtained with the detailed study performed in the 5-cell stack specifically designed to allow the variation of the individual gas supply. It has been verified that the effects caused by a moderate starvation of the reactant gases in a cell are reversible. On the contrary, the damages caused by an aggressive gas starvation, maintained for a given time, are irreversible. It has also been confirmed that the behavior of the rest of the cells was not affected during the two tests. When the voltage produced by the central cell decreased due to the gas starvation, the voltage generated by the rest of cells slightly improved. This unexpected performance is explained because the current produced by the stack is notably reduced when the potential of the affected cell is inverted. Consequently, the voltage of the unaffected cells increases to match the one corresponding to the actual current.

## Acknowledgements

Authors acknowledge the financial support of the Secretariat of State for Research of the Spanish Ministry of Economy and Competitiveness under project DPI2015-69286-C3-1-R (MINECO/FEDER, UE). Support of the Regional Government of Aragon to the Fluid Mechanics for a Clean Energy Research Group (T01\_17R) of the LIFTEC is also acknowledged.

## References

- [1] F.J. Pinar, P. Cañizares, M.A. Rodrigo, D. Ubeda, J. Lobato, *J. Power Sources* 274 (2015) 177–185
- [2] R. Taccani, T. Chinese, M. Boaro, *Int. J. Hydrogen Energy* 42 (2017) 1875–1883
- [3] C. Alegre, et al., *Int. J. Hydrogen Energy*, DOI: 10.1016/j.ijhydene.2018.07.070